Acta Cryst. (1966). **20**, 1

The Crystal Structure (at Five Temperatures) and Anisotropic Thermal Expansion of Anthraquinone

BY KATHLEEN LONSDALE, H. JUDITH MILLEDGE AND KARIMAT EL SAYED

*University College, London, W.C.*1, *England*

(*Received* 29 *March* 1965)

The structure analysis of the monoclinic single crystals of anthraquinone has been carried out at room temperature and four lower temperatures, independently. This gives molecular reorientation and the change of anisotropic thermal vibrations. Double and treble Weissenberg photographs on single films have given the anisotropic thermal-expansion figures. Over the range $+20°$ to -170 °C the principal values are

$$\alpha_{11}=56{\cdot}4;\ \alpha_{22}=125{\cdot}0;\ \alpha_{33}=-8{\cdot}6\ (\text{all}\times 10^6\ .\ °\text{C}^{-1}).$$

α_{33}, which lies very nearly along c, varies with temperature, becoming positive near to and above -12 °C. An explanation of the large expansion along the unique axis is given in terms of the large independent out-of-plane vibration of the oxygen atoms. The positive and negative α_{11} and α_{33}, and their respective magnitudes, are shown to be related to this large expansion along [010], to the molecular reorientation and thermal vibration, and to the directions of the stronger intermolecular bonds. The change of sign of α_{33} is due to the increasing effect of thermal vibration.

Introduction

The increasing use of computers in crystallographic research has made data processing and refinement of structure analyses a routine matter. With the development of automated crystal setting and recording of experimental data and the possibility of automatic trial-structure solving, the emphasis must soon shift away from the mere cataloguing of crystal structures to the value of such information in revealing or explaining biological, chemical, geological or physical processes. This will often involve the use of independent crystal-structure analyses made at various temperatures or pressures or under other changed or changing conditions such as time, varying amounts of controlled impurity, imposition of electric or magnetic fields, irradiation, different compositions of mixed molecular structures, different conditions of crystallization (pH, supersaturation) and so on.

One of the most elementary changes with temperature that takes place in a crystal structure is its thermal expansion. Except for the simplest of materials, however, very little is known about the structural relationship of expansion to thermal vibration amplitudes and other factors; and measurement of expansion coefficients is not as yet a routine part of a structure determination, although it very profitably might become so.

In order to provide data for the understanding of anisotropic thermal expansion it is not enough, however, merely to determine the crystal structure at one temperature, and the expansion figure between two temperatures. It is necessary to know how both positional and thermal atomic parameters change with changing temperature and, in the case of molecular structures, to interpret these in terms of molecular reorientation, rigid-body and non-rigid-body thermal vibrations and changes in length and direction of intermolecular bonds.

Present investigation

Preliminary discussion

The positional parameters of the atoms in anthraquinone at room temperature were determined by Murty (1960 and previous references) by means of 520 three-dimensional data, but he did not give anisotropic thermal parameters. His R value was 0.196.

All measurements have been repeated in the present work. Good small single crystals were obtained by evaporation of a benzene solution. (Crystals from chloroform were almost invariably twinned.) They did not stand grinding or shaping and had to be chosen with natural habits as nearly spherical or cylindrical as possible. Extinction was minimized by liquid-nitrogen immersion, and corrected for as far as possible by measurements of intensity on four crystals of diminishing size. The same extinction corrections (see Appendix) were used for the same crystal when measured at different temperatures, although there was some indication that the correction varied slightly with temperature. Some of the thirty strong reflexions affected by extinction were of surprisingly high θ values. The linear absorption coefficient $\mu=7.6$ cm^{-1} is small, and this correction was neglected.

Intensity measurements were made on eight equi-inclination Weissenberg photographs for hkl ($k=0,1,2,3$; $h=0$; $l=0$; $h=\pm 2l$) at room temperature, and of 1035 theoretically possible reflexions 682 had measurable values. For the measurements made at four temperatures below room temperature only the zero-level

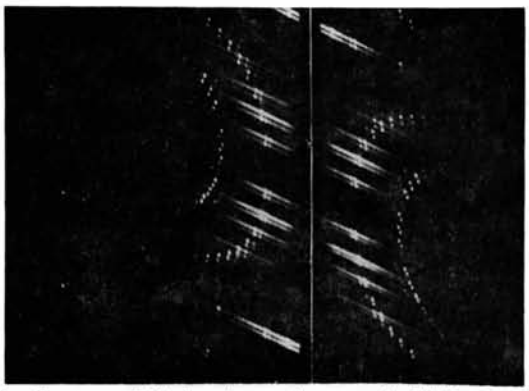

Fig. 1. Compound Weissenberg photograph, [001] as rotation axis, at temperatures +20·5 °C and −112 °C.

Weissenberg photographs (rotation axes [010] [100] [001] [10$\bar{2}$] [102]) were taken. Least-squares refinements, using Murty's parameters as a starting-point in all cases, gave final residuals

	+20.5	−12.5	−72	−112	−170 °C
R =	0.120	0.112	0.122	0.123	0.116

the refinement being stopped at the point where the recommended shifts for the atomic positional and thermal parameters were less than the estimated standard deviations. The hydrogen atoms were included but not refined, and the residuals did not include 'less-thans'. It was possible to reduce R, by the imposition of 'weights' and by other justifiable manipulation of the measured intensities, to as little as 0.059, but these adjustments were believed not to be realistic. It was decided, therefore, to take the data corresponding to the above R values and to see whether, even with this moderate degree of accuracy, the relationships between the results at the five temperatures would prove to be significant and interesting.

The temperatures below room temperature were obtained by immersion of the specimen in a stream of cold gas obtained by boiling liquid nitrogen, this stream being passed through a variable heater, somewhat above the crystal. They were measured by means of a copper–constantan thermocouple calibrated at fixed points and also placed with one junction actually inside a large anthraquinone crystal in position on the arcs in the camera, with Weissenberg motor and X-ray tube running, so that the conditions, when steady, would be as nearly as possible those of the actual experiment. Dry cold air was passed over the crystal continually to avoid the formation of ice. Care was taken to maintain the level of the liquid nitrogen in the supply Dewar, as variations in this were found to affect the prolonged steadiness of the crystal temperature. This procedure [fuller details of which have been given by El Sayed (1965)] gave controlled temperatures at any value between room temperature and −170 °C, which could be kept reasonably constant over the periods of several hours required for Weissenberg photographs. A calibration curve repeated nine months later with the same experimental set-up gave good agreement with the original.

The thermal-expansion coefficients were measured by taking Weissenberg photographs of the same crystal in the same setting and on the same film, but at two (or three) different temperatures, with a camera shift of 2 or 1.5 mm between photographs. Thus the pattern is repeated on the film, but with a slight shift (Fig. 1) and values of $\Delta\theta$ for high-angle reflexions are used for the determination of thermal expansion for every measurable reflexion in each zone. The absolute measurements of unit-cell dimensions are not of ultra-high accuracy (probably they are correct to within 0.2%, the camera and film radii having been calibrated by means of a powder photograph of an aluminum wire). The thermal-expansion coefficients are of the accuracies indicated in Fig. 8, which shows one section of the expansion figure. Measurements were made on both sides of the primary-beam trace, in order to minimize any possible mis-setting or mis-centring during the cooling process. Readings were taken with a low-powered travelling microscope (with which even the weakest spots could be seen) on all reflexions having $\theta > 20°$ and these readings were repeated independently eight times within three weeks, since it was found that humidity affected the film size in an anisotropic way. Where possible, Cu $K\alpha_1$ and α_2 spots were both used and measurements were made on the $\{h0l\}$, $\{hk0\}$, $\{0kl\}$ and $\{\bar{2}hkh\}$ zones. In particular, the expansion for the 020 reflexion had to be measured from the least three zones, since 040 was unfortunately very weak indeed and 060 unobservable.

The formula used for the calculation of the expansion coefficients was

$$\alpha = \frac{\Delta d}{d \,.\, \Delta T} \text{ where } \pm \frac{\Delta d}{d} = \frac{\operatorname{cosec}(\theta \mp \Delta\theta)}{\operatorname{cosec}\theta} - 1.$$

ΔT is the temperature range and
θ the Bragg angle corresponding to the lower temperature.

Table 1. *Unit-cell parameters, as used for purposes of structure refinement, with Δ, the extreme difference of length*

Values at −12·5°, −72°, −112° are interpolated.

Temp. (°C)	20·5 (±0·5)	−12·5 (±4·5)	−72 (±2)	−112 (±2)	−170 (±5)	Δ
a	15·83 (4)	15·81 (2)	15·76 (9)	15·74 (0)	15·69 (6)	0·144 Å
b	3·97 (1)	3·95 (8)	3·93 (3)	3·91 (6)	3·89 (0)	0·081
c	7·89 (1)	7·89 (1)	7·89 (1)	7·90 (4)	7·91 (0)	−0·019
β	102·5°	102·5°	102·5°	102·5°	102·5°	

The formula $\alpha = -(\cot\theta)\Delta\theta/\Delta T$, although sometimes given, is incorrect, because it assumes that $\Delta\theta$ is vanishingly small, whereas our aim was to make $\Delta\theta$ as large as possible.

An error of $+0.1°$ in the measurement of $\Delta\theta$ produced an error in α which was dependent upon the magnitudes of both θ and $\Delta\theta$, but which varied from 1.5% (for 20 0 $\bar{1}$ Cu $K\alpha_2$, $\theta = 85.89°$, $\Delta\theta = -4.70°$) to 24.6% (for 12 0 1 Cu $K\bar{\alpha}$, $\theta = 40.32°$, $\Delta\theta = -0.41°$).

Experimental results

The crystals are pseudo-orthorhombic (Fig. 2) but the true space group is $P2_1/a$, with two centrosymmetrical molecules of $C_{14}H_8O_2$, molecular weight 208.1 giving a calculated density 1.430 g.cm^{-3}. The unit-cell parameters were measured from rotation and inclined-beam oscillation photographs (Milledge, 1963) taken at room temperatures, those at low temperatures being

Table 2. *Orthogonal coordinates (x, y, z relative to a, b, c*) in Å for the seven carbon, one oxygen and four hydrogen atoms (the latter not refined) in the asymmetric unit, for five temperatures. Also the differences Δx_t for the extreme temperatures, as 'observed', and the corrected differences Δx_t^c derived from smoothed curves of x(y, z) versus temperature (cf.* Figs. 3, 4, 5)

	−170°C	−112°C	−72°C	−12·5°C	+20·5°C	Δx_t	Δx_t^c
C(1)							
x	1·357	1·394	1·393	1·414	1·434	0·077	0·077 Å
y	1·628	1·636	1·651	1·647	1·658	0·030	0·030
z	3·126	3·108	3·100	3·093	3·071	−0·055	−0·050
C(2)							
x	0·184	0·211	0·211	0·227	0·242	0·058	0·058
y	1·064	1·075	1·075	1·076	1·093	0·026	0·020
z	2·646	2·640	2·639	2·635	2·633	−0·013	−0·014
C(3)							
x	0·101	0·115	0·117	0·127	0·133	0·032	0·032
y	0·584	0·556	0·562	0·559	0·567	0·019	0·019
z	1·357	1·354	1·354	1·349	1·348	−0·009	−0·009
C(4)							
x	1·233	1·236	1·233	1·234	1·242	0·009	0·006
y	0·603	0·601	0·611	0·607	0·611	0·008	0·008
z	0·522	0·508	0·504	0·504	0·481	−0·041	−0·037
C(5)							
x	2·402	2·412	2·409	2·417	2·423	0·021	0·021
y	1·167	1·172	1·186	1·181	1·188	0·021	0·021
z	1·014	0·982	0·975	0·962	0·939	−0·075	−0·075
C(6)							
x	2·478	2·504	2·502	2·514	2·523	0·045	0·050
y	1·676	1·687	1·706	1·699	1·715	0·039	0·039
z	2·300	2·260	2·254	2·241	2·216	−0·084	−0·084
C(7)							
x	1·174	1·164	1·161	1·156	1·148	−0·026	−0·026
y	0·057	0·051	0·060	0·055	0·043	−0·014	−0·015
z	−0·861	−0·876	−0·880	−0·882	−0·890	+0·029	+0·030
O(8)							
x	2·173	2·155	2·150	2·143	2·132	−0·041	−0·041
y	0·102	0·096	0·109	0·101	0·091	−0·011	−0·016
z	−1·602	−1·626	−1·629	−1·640	−1·655	+0·053	+0·053
H(9)							
x	3·273	3·278	3·271	3·275	3·278		
y	1·204	1·205	1·227	1·218	1·217		
z	0·369	0·323	0·315	0·301	0·270		
H(10)							
x	3·405	3·438	3·430	3·446	3·467		
y	2·115	2·125	2·151	2·141	2·154		
z	2·664	2·612	2·602	2·588	2·550		
H(11)							
x	1·410	1·462	1·457	1·480	1·511		
y	2·022	2·038	2·053	2·048	2·073		
z	4·133	4·107	4·102	4·096	4·072		
H(12)							
x	−0·685	−0·643	−0·644	−0·627	−0·602		
y	1·020	1·033	1·033	1·034	1·056		
z	3·285	3·290	3·289	3·292	3·290		

deduced from the average thermal-expansion coefficients over the range of temperature −170° to +20.5 °C.

The fractional positional parameters and the thermal b_{ij} parameters corresponding to the temperature factor

$$\exp\{-[b_{11}h^2+b_{22}k^2+b_{33}l^2+b_{23}kl+b_{31}lh+b_{12}hk]\}$$

Table 3. *Values of observed U_{ij} referred to the molecular inertia axes L, M, N (see Table 4) for all atoms at all temperatures*

	−170°	−112°	−72°	−12·5°	+20·5 °C	
C(1)						
U_{11}	2555	2674	3063	3665	4969	10^{-5} Å^2
U_{22}	2931	4284	4561	7168	8116	
U_{33}	898	1800	2067	3179	3844	
U_{23}	−245	−270	389	483	−673	
U_{31}	396	167	201	30	753	
U_{12}	−375	−256	−46	68	−155	
C(2)						
U_{11}	2162	3123	3356	4628	5010	
U_{22}	1346	2692	3244	4282	5054	
U_{33}	1189	1664	1506	2422	3922	
U_{23}	587	371	505	66	24	
U_{31}	−359	−275	−87	217	−171	
U_{12}	278	668	330	259	−437	
C(3)						
U_{11}	1505	2430	3056	2955	4047	
U_{22}	1681	2616	2487	3322	2793	
U_{33}	1328	1651	1571	3388	2990	
U_{23}	107	170	540	434	−47	
U_{31}	−239	−111	−28	−173	434	
U_{12}	−31	−138	310	−200	−113	
C(4)						
U_{11}	2631	2590	2573	3274	4669	
U_{22}	1247	1901	2758	2790	4156	
U_{33}	1415	1445	1644	3087	3897	
U_{23}	−538	56	472	−7	−225	
U_{31}	36	8	−128	358	465	
U_{12}	−595	−84	−191	−338	−1647	
C(5)						
U_{11}	2359	3149	3312	4372	4891	
U_{22}	1156	1975	2999	2987	5361	
U_{33}	1208	1980	1663	2939	3636	
U_{23}	−12	213	355	−128	616	
U_{31}	−229	131	112	547	−162	
U_{12}	−815	−763	−1037	−857	−1942	
C(6)						
U_{11}	1760	3122	3660	3945	5271	
U_{22}	1656	3735	4522	5069	6857	
U_{33}	1562	1939	2961	3662	4090	
U_{23}	526	271	411	572	836	
U_{31}	−308	252	588	−172	598	
U_{12}	−320	−562	−1272	−500	−1506	
C(7)						
U_{11}	1779	2970	3222	3843	4992	
U_{22}	1352	2122	2565	2657	2299	
U_{33}	1316	2064	1916	3504	4567	
U_{23}	827	214	442	−133	624	
U_{31}	−424	2	−45	−4	−14	
U_{12}	39	14	−98	−408	−253	
O(8)						
U_{11}	1487	2757	3079	4341	5269	
U_{22}	1527	2207	2232	2780	9449	
U_{33}	3192	4872	5193	7434	2627	
U_{23}	144	379	746	191	−331	
U_{31}	228	−51	−152	420	−52	
U_{12}	−191	64	313	15	−427	

are given for all atoms at all temperatures by El Sayed (1965). These were used to deduce the orthogonal coordinates shown in Table 2 and the U_{ij} (Cruickshank's notation) shown in Table 3. The F_{obs} and F_{calc} for all temperatures are given in the Appendix to this paper.

Inspection of Table 2, or the actual plotting of coordinates against temperature, shows clearly that systematic errors in the experimental data have not been eliminated. One might expect a smooth variation but there is, for example, little change in x or z between

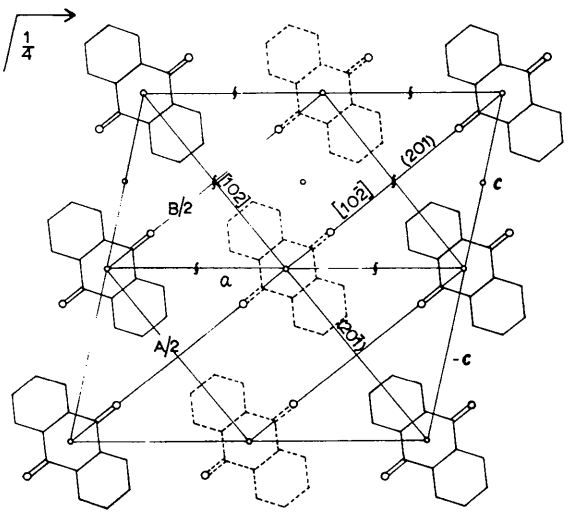

Fig. 2. Projection of structure on (010) showing both monoclinic and pseudo-orthorhombic axes; and molecular orientation, which is nearly symmetrical relative to a and c.

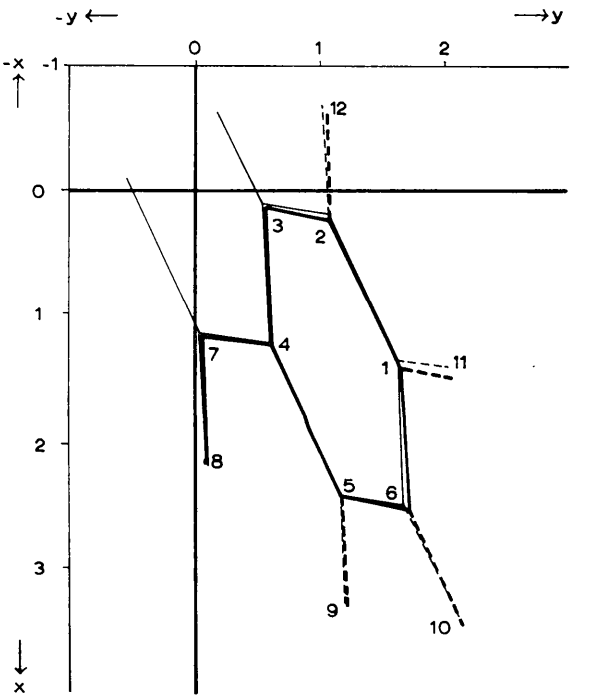

Fig. 3. Molecular orientation showing x, y in Å (see Table 2) at +20·5 (heavy line) and −170 °C (light line).

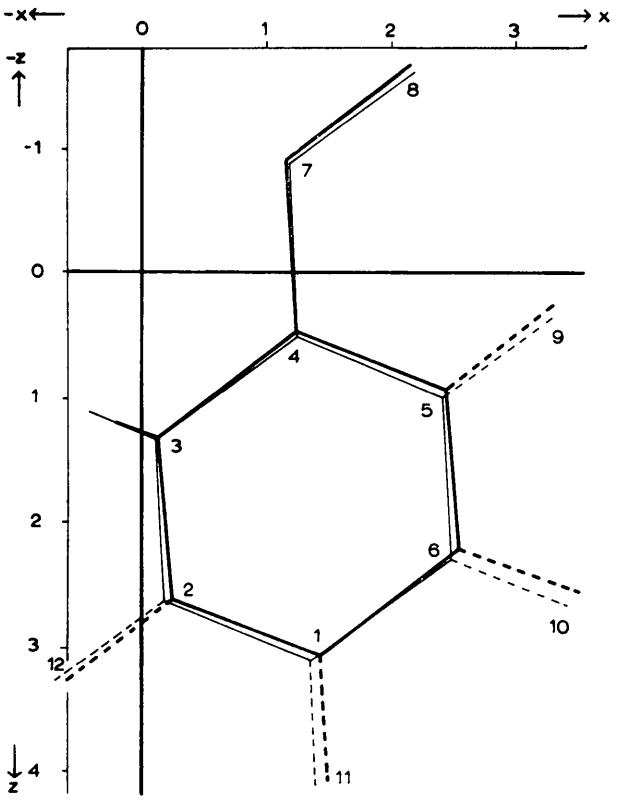

Fig. 4. Molecular orientation showing x, z in Å (see Table 2) at +20·5 (heavy line) and −170°C (light line).

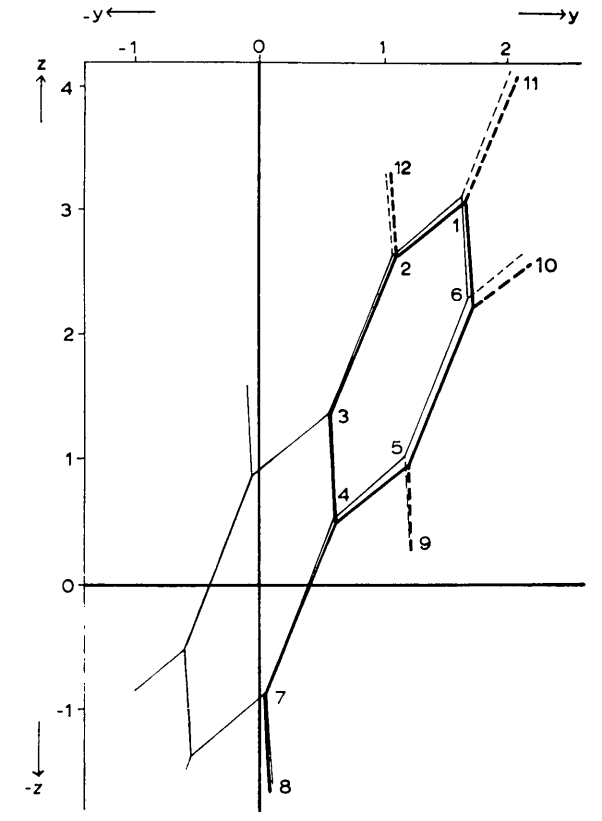

Fig. 5. Molecular orientation showing y, z in Å (see Table 2) at +20·5 (heavy line) and −170°C (light).

Table 4. *Intramolecular bond lengths and angles at different temperatures*

	−170°C	−112°C	−72°C	−12·5°C	+20·5°C	e.s.d.	Average
C(1)–C(2)	1·386	1·390	1·394	1·395	1·388	0·008	1·391 Å
C(2)–C(3)	1·392	1·390	1·387	1·389	1·395	0·008	1·391
C(3)–C(4)	1·408	1·404	1·403	1·394	1·412	0·007	1·404
C(4)–C(5)	1·388	1·390	1·391	1·392	1·396	0·007	1·391
C(5)–C(6)	1·384	1·381	1·384	1·384	1·382	0·008	1·383
C(6)–C(1)	1·394	1·396	1·396	1·392	1·384	0·008	1·392
C(3)–C(7)	1·496	1·494	1·498	1·497	1·490	0·008	1·495
C(4)–C(7)	1·488	1·492	1·492	1·494	1·486	0·008	1·490
C(7)–O(8)	1·244	1·244	1·242	1·245	1·243	0·006	1·244

	−170°C	+20·5°C		−170°C	+20·5°C
C(1)–C(2)–C(3)	121·5	120·6	C(7)–C(3)–C(2)	120·5	120·3
C(2)–C(3)–C(4)	119·2	119·8	C(7)–C(4)–C(5)	120·8	121·2
C(3)–C(4)–C(5)	118·9	118·4	C(3)–C(7)–C(4)	119·4	119·6
C(4)–C(5)–C(6)	121·7	121·4	C(3)–C(7)–O(8)	120·1	120·6
C(5)–C(6)–C(1)	120·3	120·0	C(4)–C(7)–O(8)	120·5	119·9
C(6)–C(1)–C(2)	119·4	119·8			

Table 5. *Variation of direction of the molecular inertia axes L [length C(6)—C(1′)], M (width O—O′) and N (normal to plane), with temperature, relative to a, b, c**

	−170°			−112°			−72°			−12·5°			+20·5°C		
	a	*b*	*c**	*a*	*b*	*c**	*a*	*b*	*c**	*a*	*b*	*c**	*a*	*b*	*c**
L	58·7	63·4	43·0	58·2	63·4	43·6	58·4	63·1	43·8	58·0	63·2	44·0	57·9	62·9	44·5
M	36·4	87·8	126·2	37·0	88·0	127·0	37·2	87·7	127·1	37·5	87·9	127·4	37·8	88·0	127·7
N	107·0	26·6	109·8	107·2	26·7	109·8	107·6	27·0	109·8	107·5	26·9	109·8	107·7	27·2	110·0

$-112°$ and -72 °C although there is a large change in y. It is not, therefore, the temperature measurement that is at fault. In general it appears that y for -72 °C is too large and y for -12.5 °C is too small. The small changes of molecular shape implied in the data (Table 4) are almost certainly unreal, yet taken as a whole the five sets of coordinates do give a clear and reasonable variation of molecular orientation with temperature. This shown in Figs. 3, 4 and 5 (which only show positions for the two extreme temperatures) and in Table 5 which gives the change of direction of the molecular inertia axes as the temperature changes.

If the data were sufficiently accurate one might expect to find a small lengthening of the intramolecular bond lengths as the temperature decreases (Becka & Cruickshank, 1961). These were too small to be observed. As Table 4 shows, the bond lengths are unchanged to within the estimated standard deviation. The average C—C length in the end rings is 1.392 Å, the bonds to the 'aliphatic' carbon are 1.493 Å and the C=O is 1.244 Å.

The electron-density projections on (010) at 20.5 °C and -170 °C show very marked changes of peak heights due to the changes of thermal vibration amplitudes. This is particularly true of the oxygen atoms (see Figs. 6 and 7 and Table 6). These increases may be compared with those found by Hirshfeld & Schmidt (1956) for three compounds studied at room and low temperatures.

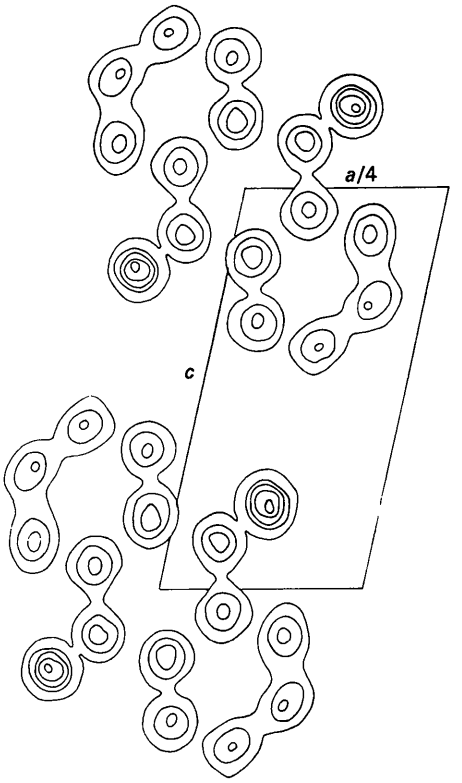

Fig. 6. (010) electron-density projection at room temperature (20·5 °C). Contours at 2, 4, 6, 8, 10 e.Å^{-2}.

The thermal-expansion experimental results are shown graphically in Figs. 8, 9 and 10 which are all to the same scale. When Fig. 9 is compared with Fig. 2 it is clearly seen that the pseudo-orthorhombic axes [102] and [10$\bar{2}$] have no significance in relation to the principal axes of expansion. These are closely related to the monoclinic axes in that α_{11} is only 1° from [100]

Table 6. *Peak values of electron density at* -170 °C *and* $+20.5$ °C (*all to within* ± 0.5) *in* e.Å^{-2}

	−170 °C	+20·5 °C		−170 °C	+20·5 °C
C(1)	7·7	6·3	C(5)	9·3	7·1
C(2)	9·3	6·9	C(6)	7·7	6·1
C(3)	7·7	7·3	C(7)	8·7	7·1
C(4)	8·5	7·1	O(8)	14·3	10·3

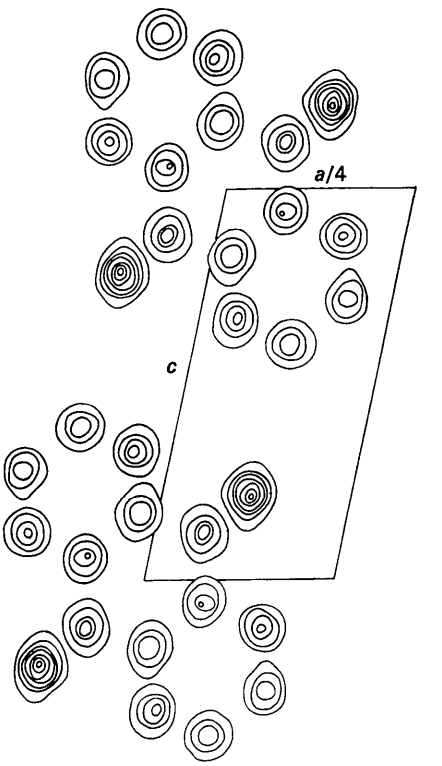

Fig. 7. (010) electron-density projection at -170 °C, showing considerable sharpening of peak heights. Contours at 2, 4, 6, 8, 10, 12, 14 e.Å^{-2}.

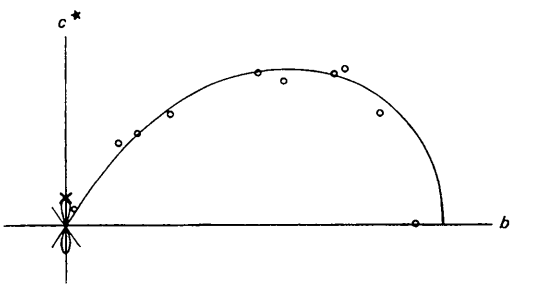

Fig. 8. Thermal-expansion coefficients normal to {0*kl*} planes. Figs. 8, 9, and 10 are on the same scale. Circles positive, crosses negative experimental values; continuous line: calculated values.

in acute β, α_{22} is of course along [010] and α_{33} is 1° from c^*, away from [001]. Their values are

$$\alpha_{11}=56.4\ \alpha_{22}=125.0\ \alpha_{33}=-8.6\ (\text{all}\ \times 10^{-6}/°\text{C})$$

taken over the whole range of temperature −170° to +20.5 °C. Comparisons of α_{ii} over various ranges of temperature show that α_{11} and α_{22} do not have much temperature variation. A compound Weissenberg photograph (Fig. 11) taken at +20.5 °C, −12.5 °C and −72 °C does show quite clearly that reflexions 208 and 207 and even 007 (for which θ is much smaller) have a smaller value of θ for *both* +20.5° and −72 °C than for −12.5 °C. In other words, the negative α_{33} becomes positive in the neighbourhood of −12 °C.

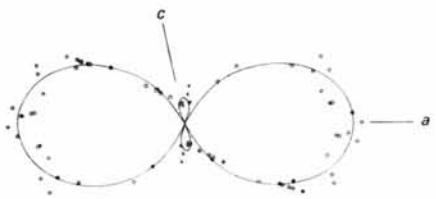

Fig. 9. Thermal-expansion coefficients normal to {*h*0*l*} planes.

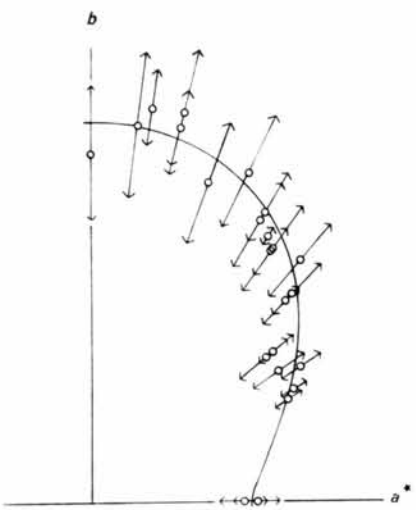

Fig. 10. Thermal expansion coefficients normal to {*hk*0} planes.

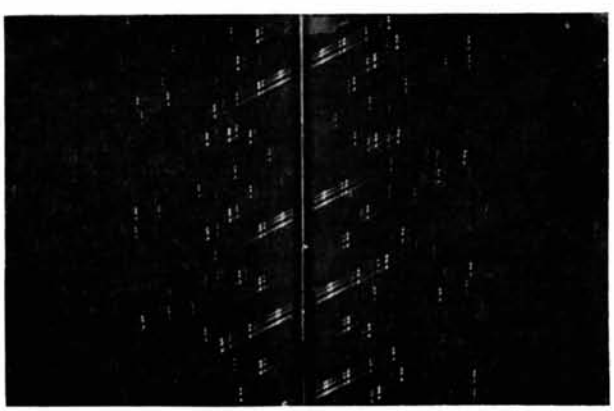

Fig. 11. Compound Weissenberg photograph taken about [010] as rotation axis; at temperatures +20·5°, −12·5° and −72 °C.

The points requiring explanation are:

(1) Why is α_{22} so large?
(2) Why is α_{11} so much larger than α_{33}?
(3) Why is α_{33} negative at low temperatures, becoming positive near to room temperature?

These questions must be answered in terms of molecular reorientations, positions of neighbouring molecules and intermolecular bonds, and thermal vibrations. Long-wave translatory vibrations, in which neighbouring molecules may be considered as moving in unison, will not be expected to contribute much to thermal expansion even though, *taken in isolation*, the molecules apparently occupy much more space at higher temperatures.

Discussion of thermal vibrations

The U_{ij} data shown in Table 3 can be treated in two ways. They can be used as they stand, with all their obvious deficiencies, to determine the molecular translations and librations at each temperature; or they can be smoothed with respect to temperature and the smoothed values used for computing*. Or indeed, if it is really believed that the molecular inertia axes L, M, N will be the principal axes of the vibration ellipsoid, then U_{ij} for C(1) and C(6) can be averaged, similarly those for C(2) and C(5), C(3) and C(4). This, however, is clearly not justified. The atomic coordinates are symmetrical with respect to L, M, N; but L, M, N are not symmetry axes in terms of the whole crystal structure; and one would not therefore expect that the principal translation axes would necessarily coincide with L, M, N. This will be seen more clearly when the lengths of intermolecular bonds are discussed.

In fact the thermal data have so far been used just as they are, without smoothing, for all computing purposes; but the effect of this is seen in Figs. 12 and 13, which show U_{33} plotted against temperature for all atoms. Fig. 12 uses the data as observed and Fig. 13 uses smoothed data. Both demonstrate clearly the outstanding values for the oxygen atom. Elsewhere (Lonsdale, Walley & El Sayed, 1966) we have shown that by treating first the whole molecule, and then the carbon atoms only, as if they were a rigid body, it is made obvious that the oxygen atoms must be executing a large out-of-plane, independent libration about the

* The magnitude and direction of B_{max}, B_{med}, B_{min} have been calculated from the b_{ij}, smoothed with respect to temperature, and unsmoothed, for all atoms at all temperatures. The e.s.d. of both magnitudes and direction cosines have been calculated with the use of a program prepared by D. Walley. In general, agreement lies within the e.s.d.'s, which at room temperature vary between 0·5 and 0·2 Å² in B. B itself varies from about 7 to 2 Å². At −170 °C the agreement is similar in magnitude but the errors are larger percentage-wise where B_{min} is very small. The smoothed and unsmoothed data for direction cosines are also surprisingly close in most cases, but in some there are large variations because of near-equality of B magnitudes (see later discussion and Table 7).

Table 7. *Magnitudes and direction cosines (relative to a, b, c*) of* B_{max}, B_{med}, B_{min} *with e.s.d. on both, for the oxygen atom at* 20.5° *and* −170 °C; *and* $\sqrt{(\overline{u^2})}$ *along* [010]

	+20·5 °C				−170 °C			
	Å²	*a*	*b*	*c**	Å²	*a*	*b*	*c**
B_{max}	7·48	−0·346	0·883	−0·316	2·55	−0·164	0·943	−0·289
B_{med}	4·21	0·405	0·445	0·799	1·34	−0·245	0·245	0·938
B_{min}	2·02	0·846	0·148	−0·512	0·98	0·956	0·225	0·191
$\sigma(B_{max})$	0·38	0·050	0·033	0·078	0·23	0·134	0·043	0·155
$\sigma(B_{med})$	0·29	0·072	0·071	0·050	0·18	0·383	0·065	0·098
$\sigma(B_{min})$	0·21	0·021	0·084	0·050	0·13	0·095	0·152	0·342
$\sqrt{(\overline{u^2})}$ [010]	0·291 Å				0·174 Å			

C(7) atoms to which they are attached. Using the carbon atoms only as a rigid body, molecular translations and librations can be deduced which when applied to the oxygen atoms, would give U_{33} calculated values as shown by the intermediate points on Fig. 13. The difference between U_{33}obs and U_{33}calc for the oxygen atoms is the measure of their independent libration. Now this out-of-plane amplitude is not far from [010]. Table 4 shows that at all temperatures the angle between *N* and **b** is ±27° for the two molecules in the unit cell.

The principal values of the thermal ellipsoids of all the atoms (deduced from observed, not smoothed, b_{ij}) with their direction cosines and the e.s.d. for both magnitudes and directions, were computed on Pegasus by means of a program prepared by Mr D. Walley. They are recorded by El Sayed (1965). From one temperature to another the magnitudes varied reasonably smoothly (compare U_{ij} in Table 3) but the direction cosines sometimes fluctuated wildly and where two of the ellipsoid axes were nearly equal the e.s.d.'s for the direction cosines were so large that the directions were indeterminate in the plane of those axes. For oxygen, however, not only the magnitudes, but also the direction cosines of the principal axes were fairly well defined at all temperatures. They are shown in Table 7, together with the value of $\sqrt{(\overline{u^2})}$ for oxygen along [010], at +20.5 °C and −170 °C only.

The values of the root-mean-square vibration amplitudes (observed, not smoothed) for all atoms at −170° and +20.5 °C along *a b c**, which are almost identical with the directions of α_{11}, α_{22}, α_{33}, are shown in Table 8 together with Δu, the increase in the r.m.s. amplitude due to the temperature rise. Our problem is to assess how much of Δu may contribute to a genuine increase of distance between a standard molecule and its nearest neighbours along [100] [010] and *c**. This is particularly difficult not only because our observed $\overline{u^2}$ are *averages*, but also because we have no idea of the distribution as between the acoustic and optical branches.

If the molecular translatory vibrations are controlled in part, at least, by the configuration of the nearest neighbours, and the librations by the inertia of the molecule itself, then it might be reasonable to suggest that the translations are the more likely to be of long wavelengths and to involve coordinated movements of

Table 8. *Root-mean-square amplitudes* $\sqrt{(\overline{u^2})} = (B/8\pi)^{\frac{1}{2}}$, *observed, along* α_{11}, α_{22}, α_{33}, *at* −170° *and* +20.5 °C

		$a(\alpha_{11})$	$b(\alpha_{22})$	$c^*(\alpha_{33})$
C(1)	−170 °C	0·152	0·117	0·159 Å
	+20·5 °C	0·260	0·215	0·235
	Δu	0·108	0·098	0·076
C(2)	−170 °C	0·123	0·107	0·139
	+20·5 °C	0·215	0·200	0·232
	Δu	0·092	0·093	0·093
C(3)	−170 °C	0·125	0·109	0·131
	+20·5 °C	0·173	0·188	0·182
	Δu	0·048	0·079	0·051

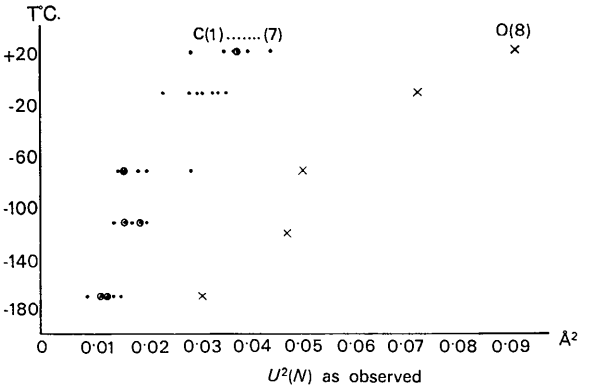

Fig. 12. U_{33}obs $[\overline{u^2}(N)]$ plotted against temperature, for all atoms.

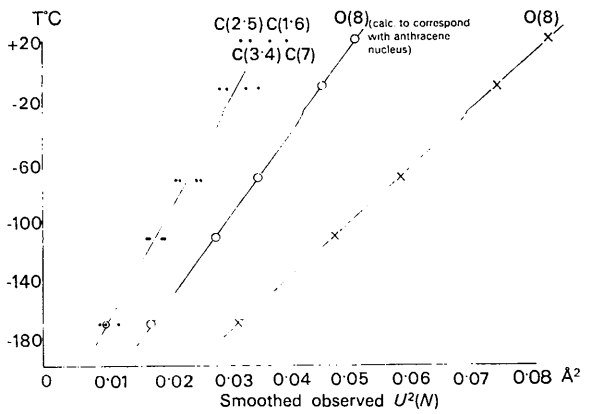

Fig. 13. The same as Fig. 12 but using smoothed values of U_{33}.

Table 8 (*cont.*)

		$a(\alpha_{11})$	$b(\alpha_{22})$	$c^*(\alpha_{33})$
C(4)	−170°C	0·116	0·128	0·151
	+20·5°C	0·168	0·209	0·235
	Δu	0·052	0·081	0·084
C(5)	−170°C	0·094	0·111	0·162
	+20·5°C	0·178	0·193	0·264
	Δu	0·084	0·082	0·102
C(6)	−170°C	0·111	0·118	0·153
	+20·5°C	0·208	0·220	0·267
	Δu	0·097	0·102	0·114
C(7)	−170°C	0·111	0·106	0·144
	+20·5°C	0·165	0·216	0·210
	Δu	0·054	0·110	0·066
O(8)	−170°C	0·115	0·174	0·135
	+20·5°C	0·196	0·291	0·224
	Δu	0·081	0 117	0·089

Table 9. *Values of T_{ij}, ω_{ij} (Cruickshank's notation) calculated on the basis of the whole molecule as a rigid body, for all five temperatures*

(All from unsmoothed data)

T_{ij} ($\times 10^{-4}$ Å^2)	−170°C	−112°C	−72°C	−12·5°C	+20·5°C
T_{11}	194	262	289	347	430
T_{22}	135	204	239	270	298
T_{33}	100	108	86	240	264
T_{23}	+17	+28	+57	+7	+7
T_{31}	−16	+5	+9	+8	+46
T_{12}	−25	−13	−21	−24	−81
ω_{ij} ($\times 10^{-5}$ radians^2)					
ω_{11}	274	496	546	623	888
ω_{22}	0	29	78	22	41
ω_{33}	48	120	144	218	309
ω_{23}	−1	+20	+17	−22	−7
ω_{31}	−26	+20	+16	−40	+122
ω_{12}	−24	−16	−38	−36	−6

Table 10. *Values of T_{ij}, ω_{ij} calculated for +20.5° and −170 °C only, from data smoothed with respect to temperature, for a rigid-body composed of* (*a*) C(1)—C(6) *only* (*b*) C(1)—C(7) only (*c*) *the whole molecule*

		T_{11}	T_{22}	T_{33}	T_{23}	T_{31}	T_{12}	($\times 10^{-5}$Å^2)
a)	+20·5°C	423	302	334	18	35	−64	
	−170°	198	113	104	14	−12	−15	
		ω_{11}	ω_{22}	ω_{33}	ω_{23}	ω_{31}	ω_{12}	($\times 10^{-5}$ Å^2)
	+20·5°C	−16	5	30	1	8	−2	
	−170°	−6	1	8	0	−2	−3	
(*b*)	+20·5°C	420	292	340	19	34	−59	
	−170°	196	130	105	28	−14	−12	
	+20·5°C	7	2	30	0	8	−2	
	−170°	−4	1	6	1	−2	−3	
(*c*)	+20·5°C	408	303	246	15	34	−54	
	−170°	188	147	64	32	−14	−10	
	+20·5°C	82	5	28	−1	6	−2	
	−170°	29	2	4	1	−3	−3	

neighbouring molecules. They would then contribute *least* to thermal expansion. This does seem to be the case. Table 9 shows the values of T_{ij} and ω_{ij} (Cruickshank's notation) at all temperatures, based on the rigid-body analysis, using all atoms. (Using the seven carbon atoms only (see Table 10), the values for $i \neq j$ are not much changed, the main change being in T_{33} and ω_{11}). A fair deduction from the cross-term values seems to be that the principal molecular librations are very near to the inertia axes, but that the principal molecular translations are not so near and are more dependent on the directions of intermolecular bonds, as they were also, for example, in diketopiperazine (Lonsdale, 1961). In that case the translations can, to a first approximation, be discounted in assessing the contribution of the thermal vibrations to thermal expansion. In the direction of [010], that is, of α_{22}, the observed value of $\sqrt{(\overline{u^2})}$ is greatly enhanced by the independent out-of-plane libration of the oxygen atom.

Thermal variation of intermolecular bond lengths

In addition to knowing the changes of molecular orientation, it is important to know how the intermolecular bond lengths change, in order to assess the importance of reorientation and changed thermal vibration amplitudes in respect of thermal expansion. Table 11 gives a list of the lengths at the five temperatures of all intermolecular bonds less than 3.7 Å in length at +20.5 °C. Table 12 gives their direction cosines at −170° and +20.5 °C only. It will be seen that, apart from one bond, they all increase in length. The question is, whether the components of these changes in length of intermolecular bonds can be understood in terms of molecular reorientation combined with some part of the molecular thermal vibration. The simplest case is that of the large expansion along the *b* axis: α_{22} is 125.10^{-6} . °C^{-1} and there are eight independent short intermolecular bonds between each pair of molecules along the [010] direction.

Figs. 4 and 5 show that the molecular reorientation involves the atoms C(6) and its attached H(10) in the maximum movement in the [010] direction. The change Δy from −170° to +20.5 °C is almost 0.039 Å for both and therefore the total increase of space parallel to [010] taken up by the centrosymmetrical molecule in turning is ∼0.078 Å. At the same time, however, the molecule turns so that Δy for the oxygen atom is −0.016 Å and in respect of its width, therefore, the molecule occupies 0.032 Å *less* space along [010]. It is difficult to see what effect these combined movements would have in altering the packing arrangements of the identical array of molecules along [010]. A more useful consideration is that of Δy for the atoms which take a major part in the intermolecular bonds along [010]. The maximum bond changes are those between C(1) of the molecule at 000 and C(2) of that at 010 (0.076 Å) and also between C(2) (000) and C(3) (010) (0.073 Å). For C(1), Δy=0.030 Å, but for C(2), Δy=

0.020 Å *in the same direction;* hence the change of orientation only accounts for 0.010 Å of the actual 0.076 Å increase which occurs. Similarly Δy[C(2) (000)] —Δy[C(3) (010)] is nearly zero, yet an increase of bond length of 0.073 Å occurs. For C(5) (000) and C(4) (010) the molecular reorientation only accounts for 0.013 Å of the observed bond increase of 0.070 Å along [010]. Although the accuracy of any individual bond length or Δy measurement does certainly not justify the use of the third decimal place, yet the accumulated effect of the above considerations is that there is an increase of intermolecular bond length along [010] from −170° to +20.5 °C of about 0.06 Å, not accounted for by molecular reorientation. This is only a fraction of the increase in $\sqrt{(\overline{u^2})}$ along [010], which changes from 0.11_4 Å at −170 °C to 0.20_6 Å at +20.5 °C for the atoms C(1) to C(7) (±0.015 for individual atoms) and from 0.17_4 Å to 0.29_1 Å for oxygen over the same temperature range. It is clear that even though, as previously suggested, the long-wave acoustic vibrations will contribute little to the expansion, yet the contribution of the librational vibrations and particularly that of the oxygen atoms (whose total mean vibration amplitude $2\sqrt{(\overline{u^2})}$ increases from 0.35 Å to 0.58 Å) is sufficient to account for the expansion of the intermolecular bonds and hence of the *b* axis.

The difference in the values of α_{11} and α_{33} is more difficult to explain. As Fig. 2 shows, the molecular orientation is nearly symmetrical relative to *a* and *c*. From Table 2 it will be seen that the reorientation with temperature causes the following maximum coordinate changes (− 170°C to + 20.5°C)

C(1) $\Delta x = +0.077$ Å	C(6) $\Delta z = -0.084$ Å
O(8) $\Delta x = -0.041$ Å	O(8) $\Delta z = +0.053$ Å

Again, it is difficult to see how this reorientation may be expected to affect packing considerations, and it is more helpful to consider the changes of intermolecular

Table 11. *Intermolecular bond lengths* (< 3.7 Å) *at all temperatures**

			−170°	−112°	−72°	−12·5°	+20·5 °C
000	C(1)–C(2)	010	3·562	3·588	3·589	3·618	3·635
	–C(3)	010	3·550	3·571	3·572	3·596	3·600
000	C(2)–C(3)	010	3·609	3·634	3·654	3·674	3·679
000	C(4)–C(7)	010	3·619	3·640	3·654	3·678	3·670
000	C(5)–C(4)	010	3·560	3·578	3·589	3·614	3·623
	–C(7)	010	3·571	3·581	3·588	3·607	3·600
000	C(6)–C(4)	010	3·557	3·562	3·568	3·587	3·587
	–C(5)	010	3·618	3·634	3·647	3·672	3·674
000	C(1)–O(8)	001	3·478	3·491	3·483	3·489	3·513
000	C(2)–O(8)	001	3·617	3·595	3·577	3·571	3·564
000	C(5)–O(8)	$\frac{1}{2}\frac{1}{2}0$	3·439	3·479	3·504	3·531	3·550
000	C(6)–O(8)	$\frac{1}{2}\frac{1}{2}0$	3·293	3·294	3·312	3·327	3·330

* Objection may be taken to the use of the word *bond* in this sense. However, the main property of the crystal is that the molecules are *held together* in an almost static pattern which requires the expenditure of energy to break it up. We believe, therefore, that the use of the term *intermolecular bond* is justified.

Table 12. *The direction cosines of the shortest intermolecular bonds and L, the principal component of each such bond, at* −170° *and* +20.5 °C (*relative to a, b, c**)

				a	*b*	*c**	*L*
000	C(1)–C(2)	010	−170 °C	−0·329	0·935	−0·135	3·330
			+20·5°	−0·328	0·937	−0·120	3·406
000	C(1)–C(3)	010	−170°	−0·354	0·792	−0·498	2·814
			+20·5°	−0·361	0·800	−0·479	2·880
000	C(2)–C(3)	010	−170°	−0·023	0·934	−0·357	3·370
			+20·5°	−0·030	0·936	−0·349	3·443
000	C(4)–C(7)	010	−170°	−0·016	0·924	−0·382	3·345
			+20·5°	−0·026	0·927	−0·374	3·402
000	C(5)–C(4)	010	−170°	−0·328	0·934	−0·138	3·325
			+20·5°	−0·326	0·937	−0·126	3·395
000	C(5)–C(7)	010	−170°	−0·344	0·778	−0·525	2·780
			+20·5°	−0·354	0·785	−0·508	2·826
000	C(6)–C(4)	010	−170°	−0·350	0·792	−0·500	2·818
			+20·5°	−0·357	0·799	−0·484	2·843
000	C(6)–C(5)	010	−170°	−0·021	0·934	−0·355	3·380
			+20·5°	−0·027	0·937	−0·347	3·443
000	C(1)–O(8)	001	−170°	−0·258	−0·439	0·861	2·995
			+20·5°	−0·287	−0·446	0·847	2·975
000	C(2)–O(8)	001	−170°	0·077	−0·267	0·961	3·476
			+20·5°	0·051	−0·281	0·958	3·415
000	C(5)–O(8)	$\frac{1}{2}\frac{1}{2}0$	−170°	0·952	0·256	0·171	3·278
			+20·5°	0·947	0·250	0·202	3·361
000	C(6)–O(8)	$\frac{1}{2}\frac{1}{2}0$	−170°	0·971	0·113	−0·212	3·196
			+20·5°	0·980	0·108	−0·168	3·263

distance along each direction. There are only two intermolecular bonds along each of the [100] and [001] directions less than 3.7 Å in length. The point of major significance is that along [100] the connection is between a molecule and its *reflexion*, while along [001] the connection is between two *similar* molecules. Now the molecule itself is centrosymmetrical, and the situation is therefore as shown in Fig. 14 and Table 12. As the standard molecule at 000 swings round, the tendency is for the bond (000) C(6)—O(8′) ($\frac{1}{2}\frac{1}{2}$0), which is the shortest bond near to [100], to swing even nearer; so that its projection along [100] lengthens more than the actual bond lengthens. The increase of 0.072 Å in $\frac{1}{2}a$ cannot be accounted for, however, by the reorientation of the molecules alone. This reorientation causes a change of Δx of +0.050 Å for O(6) of 000 and of +0.041 Å for the centrosymmetrical O(8′) of the molecule at $\frac{1}{2}\frac{1}{2}$0 (since the value of Δx for O(8) is −0.041 Å). The reorientation of the molecules therefore causes a shift of position of the (000) C(6) to O(8′) ($\frac{1}{2}\frac{1}{2}$0) bond, but not necessarily of the molecules relative to each other. There is, however, a considerable change in the thermal vibration amplitudes of C(6) and O(8′) from −170 °C to +20.5 °C, and Fig. 14 shows that the disposition of the intermolecular bonds along [100] is such that, although long acoustical waves may be neglected as a cause of thermal expansion, yet any short or optical vibrations must cause an increasing separation of the molecules along that direction. The maximum change in root-mean-square amplitudes along [100] for C(6) and O(8′) is 0.097+0.081=0.178 Å (from Table 8), whereas the increase in the C(6)—O(8′) bond component along [100] (from Table 12) is 0.067 Å, only a fraction of that amount.

By contrast, Table 12 shows that although the intermolecular bond nearest to [001], that from (000) C(2) to O(8) (001), hardly changes its direction at all with temperature, yet its component along [001] is decreased by 0.061 Å as the temperature rises from −170 °C to +20.5 °C. The reorientation of the molecules causes a change of $\Delta z = -0.014$ in C(2) and of −0.053 in the coordinate (originally 6.255 Å) O(8) of 001. This does account for a good part of the change in intermolecular bond length. The remainder reflects the change of −0.019 Å in the c axis. Fig. 14 shows that as long as the thermal vibrations along [001] are not too large, any expansion along [010] is bound to be accompanied by a contraction along [001] because of the trellis-work nature of the intermolecular bonds in that direction. As the thermal vibrations increase in magnitude those of the optical type are bound to increase the distance between the molecules and to turn the contraction along [001] into an expansion.

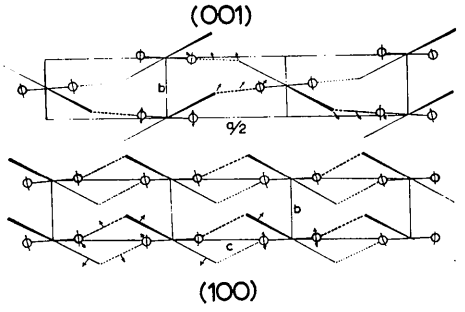

Fig. 14. Diagrammatic representation of intermolecular bonds in the (001) and (100) projections. Vibrating O atoms are shown by circles, intermolecular 'bonds' by dotted lines. The small arrows show relative directions of movement as the temperature increases.

It is probable that a consideration of H—H and of H—O contacts would yield useful information, but for such results to be really significant the data (at different temperatures) should be extended to anthrone ($C_{14}H_{10}O$) which is closely isostructural with anthraquinone ($C_{14}H_8O_2$) although CH_2 has replaced half the CO groups in a partially disordered way. This is a major research and would need well-established H positions, and hence much better as well as more-extended experimental data than are used here.

APPENDIX
Experimental data

R values of 12% do not by any means represent the limit of accuracy attainable with good photographic data, and require some explanation in view of the considerable number of conclusions deduced in this paper. The principal cause of experimental inaccuracy was uneven spot-shapes in the $h0l$ data owing to the impossibility of grinding spheres. The other four zones used had to be scaled together *via* the $h0l$ data alone, since there are virtually no $0k0$ reflexions. Furthermore, four different crystals had been used to collect the zones of data owing to difficulties of re-mounting, and these crystals required different extinction corrections. Hence the uncorrected intensities did not scale well together in any case.

Accordingly, all five sets of data at the different temperatures were refined independently to about $R=14\%$. For each set structure factors were calculated for a regular molecule oriented along the inertia axes derived from the coordinates at that stage of refinement. The five zones of data were then scaled to the calculated structure factors, only those observed values being used which were weak enough for extinction to be negligible. With these scales, a value of the extinction parameter β in the expression $I_{TRUE}=I_{OBS}+\beta I^2_{OBS}$ was obtained (assuming $I_{TRUE}\simeq I_{CALC}$) for each crystal so as to give reasonable corrections for the appropriate zone at all five temperatures. The final cycles of refinement were then carried out with the data corrected in this way. It can be seen from Table 13* that the agreement is much better for zones other than $h0l$, because spot-shapes were much more uniform in the other zones.

* It will be seen that the computer prints F(obs) with the sign found for F(calc).

Table 13. F_{obs} *and* F_{calc} *at five temperatures*

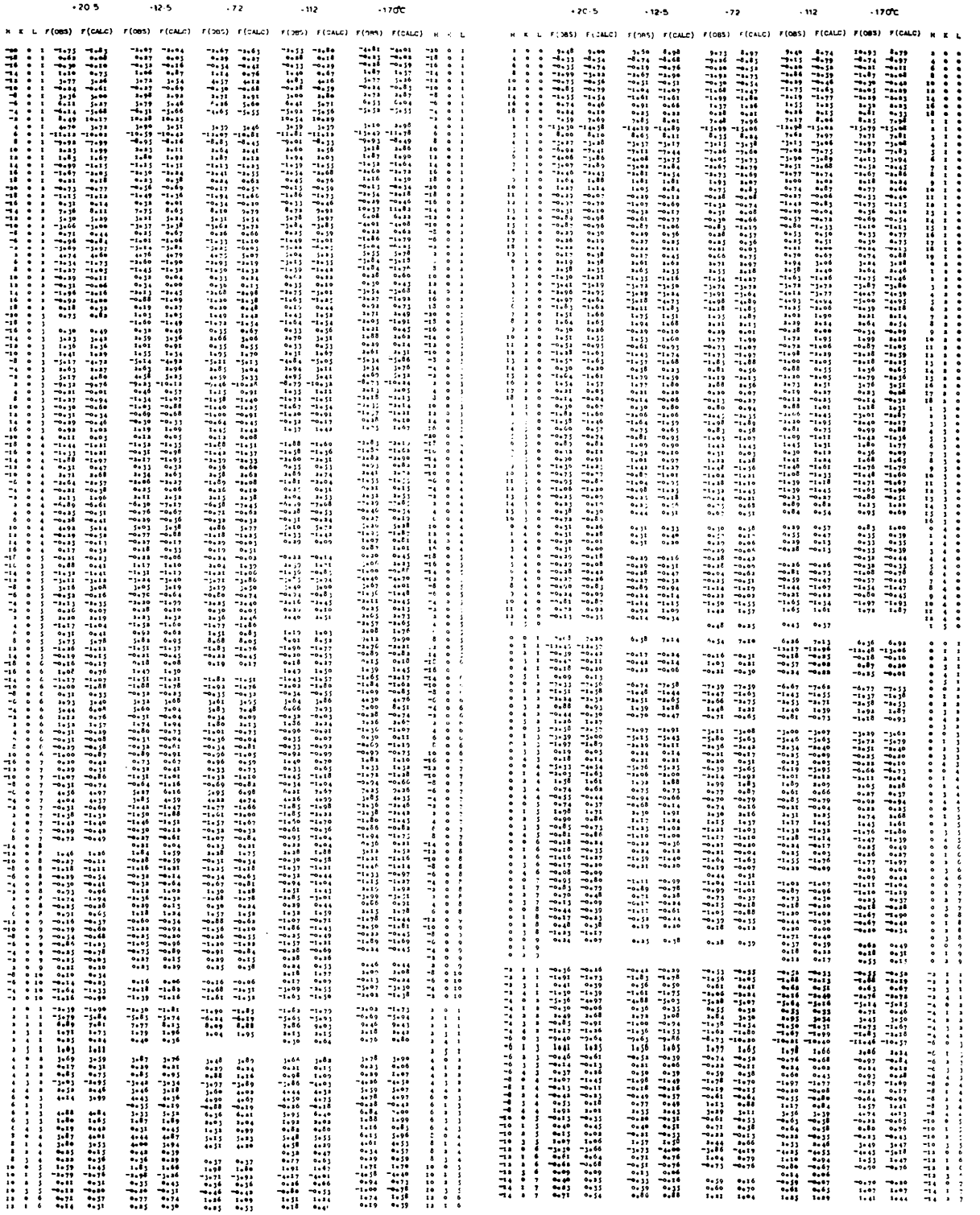

The observed intensities for each zone were scaled together and processed by means of a least-squares program (Milledge & Walley, to be published) which proved very efficient in eliminating gross errors of indexing, intensity estimation and punching, as well as providing experimental weights. These weights were in fact used in the refinement, but are not likely to have had a very large effect on the final result since there was already a fairly even distribution of ΔF values among the observed reflexions. The results appear to indicate that *molecular orientations* derived from inertia calculations on coordinates obtained by refining relatively inaccurate data do have a much greater significance than the coordinates themselves. All estimates of errors derived from these diagonal SFLS refinements are certainly lower limits.

One of us (K. El S.) wishes to acknowledge with thanks the award of a research scholarship by the Ein-Shams University, Cairo, U.A.R. A grant from the Department of Scientific and Industrial Research has helped to provide computing facilities and apparatus; we are also indebted to Ferranti Ltd and to International Computers and Tabulators for the gift and servicing of the computer PEGASUS on which the greater part of the computing was carried out. Dr B. V. R. Murty very kindly sent us his lists of uncorrected intensities at room temperatures for comparison with our own.

Renferences

BECKA, L. N. & CRUICKSHANK, D. W. J. (1961). *Acta Cryst.* **14**, 1092.
EL SAYED, K. (1965). Thesis, London.
HIRSHFELD, F. L. & SCHMIDT, G. M. J. (1956). *Acta Cryst.* **9**, 233.
LONSDALE, K. (1961). *Acta Cryst.* **14**, 37.
LONSDALE, K., WALLEY, D. & EL SAYED, K. (1966). *Acta Cryst.* **20**, 13.
MILLEDGE, H. J. (1963). *Acta Cryst.* **16**, 72.
MURTY, B. V. R. (1960). *Z. Kristallogr.* **113**, 445.

Acta Cryst. (1966). **20**, 13

Methods of Testing for Independent Vibrations of Atoms in a Molecule, Illustrated by Anthraquinone

BY KATHLEEN LONSDALE, D. WALLEY AND KARIMAT EL SAYED
*University College, London, W.C.*1. *England*

(*Received* 29 *March* 1965)

Thermal coefficients have been measured for anthraquinone at five different temperatures. These indicated that the oxygen atom possessed a large independent out-of-plane libration. This was confirmed by treating first the whole molecule and then the anthracene nucleus alone as if they were rigid bodies, and noting the *differences* in the **T**, **ω** values thus determined. These were particularly large for ω_{11}. This method of using successively smaller parts of the molecule as a basis for a rigid-body thermal analysis seems capable of extension to more complicated molecules. A critical consideration of the individual values of $(U \text{ obs} - U \text{ calc})_{ii}$ may also reveal large discrepancies which are consistent at different temperatures, even when the *average* value is similar to the e.s.d. for the experimental data. Such an inspection has revealed a translatory vibration of the anthracene nucleus along the inertia axis L, relative to the oxygen atom. This may be a consequence of the strong intermolecular C(6)(000) --- O(8)($\frac{1}{2}\frac{1}{2}$0) bond, combined with the large out-of-plane O(8) libration. There is no sign of any accompanying out-of-plane libration of the outer carbon atoms, such as would be expected for a 'butterfly' motion.

During an investigation of the crystal structure, thermal vibrations and thermal expansion of anthraquinone, for which measurements were made at five temperatures (Lonsdale, Milledge & El Sayed, 1966) it was noticed that the thermal vibration of the oxygen atoms normal to the molecular plane (Fig. 1) was rather larger at all temperatures than would have been expected by comparison with the remainder of the molecule. In order to test whether this could conceivably be due to a particularly large libration about the L axis the values of the U_{ij} were computed and hence the **T**, **ω** matrices (Cruickshank's notation), with a program written for Pegasus by one of us (D.W.).

The calculations were carried out:

(1) For the whole molecule, which is centrosymmetrical.
(2) For the anthracene nucleus alone, omitting oxygen atoms.

If the rigid-body hypothesis were adequate, then the **T**, **ω** matrices obtained for (1) and (2) should be effectively identical. In fact they were very different, the main difference being that the presence of the oxygen